

## ENVIRONMENTALLY ADAPTIVE SONAR

Ole J. Lorentzen<sup>a</sup>, Stig A. V. Synnes<sup>a</sup>, Martin S. Wiig<sup>a</sup>, Kyrre Glette<sup>b</sup>

<sup>a</sup> Norwegian Defence Research Establishment (FFI), P.O. box 25, NO-2027 KJELLER, Norway

<sup>b</sup> University of Oslo, P.O. box 1080 BLINDERN, 0316 OSLO, Norway

Contact author: Ole J. Lorentzen, P.O. box 25, NO-2027 KJELLER, Norway, e-mail: Ole-Jacob.Lorentzen@ffi.no (fax: +47 63 80 71 15)

**Abstract:** *Active sonar operations in shallow waters are important both for autonomous underwater vehicles (AUV) with synthetic aperture sonar (SAS) or sidescan sonar, and for hull-mounted forward-looking sonar. One of the challenges in shallow water operations is that the direct bottom return is often contaminated by other signal returns, either from scattering off both surface and bottom, or by direct surface backscattering. The contributions of different multipaths depend on the sensor depth, the vertical beam patterns and the environment. In this paper we present a method for adapting the sonar parameters to the environment in order to minimize the multipath contamination.*

*The method is developed for AUV-mounted interferometric sidescan sonar systems, supporting depth estimation using two vertically displaced receiver arrays. The relative time delay of the direct signal and the multipath signals will differ between the two arrays. This allows for a measure on the degree of multipath contamination as a bi-product of the depth estimation. We use these measurements to calibrate a simulator which predicts the strength of both the direct signal return and each multipath return in the measured environment. The simulator is then rerun with different sonar settings in a search for minimum multipath contamination.*

*The method is demonstrated on data recorded with the HISAS 1030 sonar on a HUGIN 1000 AUV developed by the Norwegian Defence Research Establishment (FFI) and Kongsberg Maritime. The best sensor depth and steering of the 16-element vertical transmitter array is suggested. This allows for in situ adaptation to the environment, and also provides validation of the suggested settings.*

**Keywords:** *adaptive sonar, adaptive transmit beam, autonomy, sonar performance modelling, AUV, sidescan sonar*

## 1. INTRODUCTION

We investigate a concept for automatic adaptation of sonar settings to the environment by calibrating a model to a measurement and simulating the performance with other sonar settings. The sonar system consists of an interferometric HISAS 1030 sonar on a HUGIN autonomous underwater vehicle (AUV), see Figure 1.



**Figure 1:** A HUGIN 1000 AUV.

When a sidescan sonar is used in shallow water, i.e. where the depth is less than half the maximum sonar range, multiple reflections off the sea floor and sea surface may interfere with the direct signal return from the sea floor [1]. An example of how severe such multipath induced image degradation can be is shown in Figure 2. Without a large vertical array, we cannot use beam forming to prevent this. In very shallow water, the multipath's angle of arrival may be very similar to the direct signal return, which would require a prohibitively large vertical array to create a narrow beam. This, in turn, would require detailed a priori knowledge of the scene bathymetry in order to find the correct direction of arrival. Instead, we propose to adapt the transmit beam in order to limit the generation and strength of the multipath signals. For this purpose the HISAS 1030 has a 16-element vertical array transmitter, which creates a defocused beam with controllable width and direction.

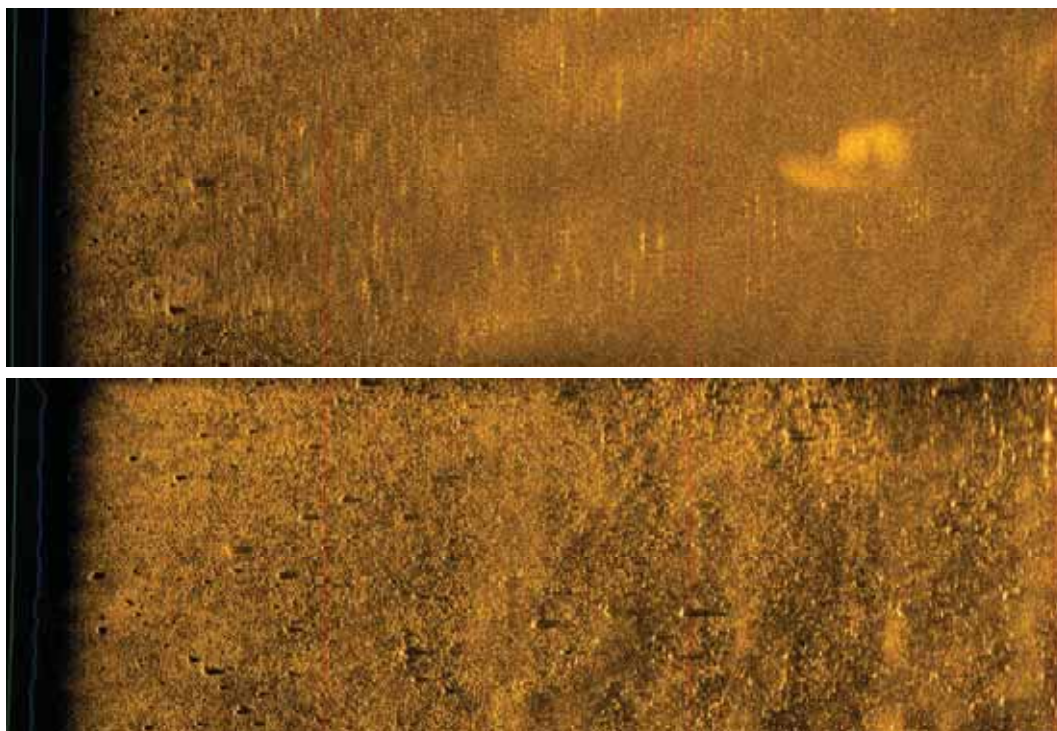


**Figure 2:** Example of a seabed on the coast of Horten, Norway, where we have imaged the same scene twice with the same sonar settings, but on different dives about six days apart. Vertical red lines mark the range every 50 meters. The upper image shows severe degradation, primarily caused by multipath, and features low bathymetric coherence compared to the lower image. The AUV depth is 2.8 meters, and the total sea floor depth is 9.8 meters. The upper image is collected with winds of about 3 m/s from south-southwest, while the lower image was collected with winds of about 10 m/s from south, reported from the nearest meteorological observation station.

Our concept for the environmentally adaptive sonar process is illustrated in Figure 3. First, a measurement is collected and processed for sidescan bathymetry and bathymetric coherence [2]. The coherence is used to estimate a measured signal to noise ratio (SNR). The bottom type and surface state is estimated by fitting a simulated SNR from a sonar performance model to the measured SNR. With these environment parameters resolved, the sonar performance model is used to simulate performance using other sonar parameters, and even other measurement geometries, like different vehicle altitudes. We use the swath width to compare new solutions to the measurement, defined here as the length of the largest continuous range-segment with SNR larger than 0 dB. Finally, if the best swath width simulated with new settings is an improvement, we apply these sonar settings for the next measurement.

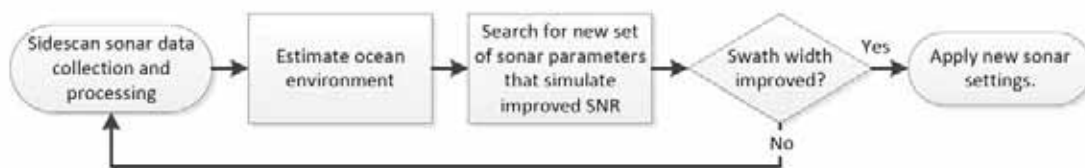


**Figure 3:** Flowchart describing the adaptive sonar process. A sonar performance model is used both for estimating the ocean environment and for simulating the SNR with various sonar parameters.

## 2. SONAR PERFORMANCE MODEL

We need a sonar performance model to provide parameters that describe the environment, and to predict the sonar performance with different sonar settings. For this purpose we have used the modeling software SMURF [3], developed by the Norwegian Defence Research Establishment (FFI).

The SMURF model is a 2-dimensional (depth and range) ray tracing model for sonar performance, particularly developed for shallow water. In order to simulate the path of sound in the water, many different aspects of how pressure waves travel through viscous media need to be considered. The most significant factors are refraction, multiple specular and diffuse reflections (scattering) off the sea floor and surface, and attenuation and geometrical spreading in the water. In addition, the beam patterns of the transmit and receive antenna arrays are significant.

## 3. METHOD

The result of the simulation in the sonar performance model SMURF is a simulated SNR. In order to resolve the environmental parameters, i.e. the bottom type of the sea floor and the roughness of the sea surface, we tune these and compare the simulated SNR to the measurement until we find a good fit between the simulated and measured SNRs.

The measured SNR is estimated from the bathymetric coherence, which is the normalized cross-correlation of the two coregistered images from the interferometric HISAS 1030 sonar setup [1,4]. High coherence means more coherent signal energy, which will be the direct signal return since the angle of arrival matches between the two coregistered images. Low coherence means more noise, which comprise the multipath returns since they don't have the same angle of arrival as the direct signal return, and thus will not be coherent in the coregistered images.

The bathymetric coherence,  $|\gamma|$ , of the two coregistered images is calculated by finding the peak value in the coherence function  $\gamma(\tau)$

$$|\gamma| = \max_{\tau} |\gamma(\tau)|,$$

where  $\tau$  is the time lag applied to one of the signals in the coherence function. This is to say that the phase shift which results in the maximum total coherence between the two measured signals is the shift that makes them coregistered. This coherence has a known bias towards higher values because the correlation is performed with data series of a finite number of samples. An expression for the variance exists, and shows that the bias increases with decreasing number of samples [4,5].

An estimate of the SNR in a sonar image can be expressed by the coherence as [4]

$$SNR = \frac{|\gamma|}{1-|\gamma|}.$$

In shallow water, where the main cause of signal degradation is multipath, this SNR estimate is a good measure of signal to multipath ratio [3].

In order to search for new and improved sonar parameters, the model must be calibrated to match the current environment. This calibration is a search for fitting environmental parameters, i.e. bottom type and sea state. The sonar settings and geometry are input, as well as the measured sound speed profile and the measured sidescan bathymetry. Then, the two environmental parameters are varied to simulate SNR results with different combinations of bottom types and sea states. The measured SNR estimate is then compared to these simulated SNRs with varying environmental parameters. The best fit in the least squares sense between the measured and simulated SNRs is selected. This is implemented by discretizing the sea states and performing a greedy search algorithm in the bottom type dimension, and selecting the best result found.

Using the now calibrated model, we investigate new settings by performing a search for improved simulated performance by using the sonar settings as variable parameters. We test both a brute force search, trying all solutions for analytic purposes, and a hill climbing algorithm, for shorter runtime.

The brute force search was performed for beam widths from 10 to 80 degrees in steps of 5 degrees, and electronic beam steering of -60 to 40 degrees in steps of 5 degrees, positive down from the horizon. In addition to the electronic steering, the sonar array is mounted with a mechanical direction of 22 degrees down from the horizon.

The hill climbing algorithm was allowed to use beam widths from 10 to 80 degrees, electronic beam steering of -50 to 20 degrees, and altitudes from minimum 3 meters above the sea floor up to maximum 80 meters above the sea floor, though never less than 2 meters depth. The reason for slightly reducing the set of available steering angles compared to the brute force search was simply that the extreme values direct the beam too far away from the scene, and thus only contribute to increasing the runtime of the algorithm.

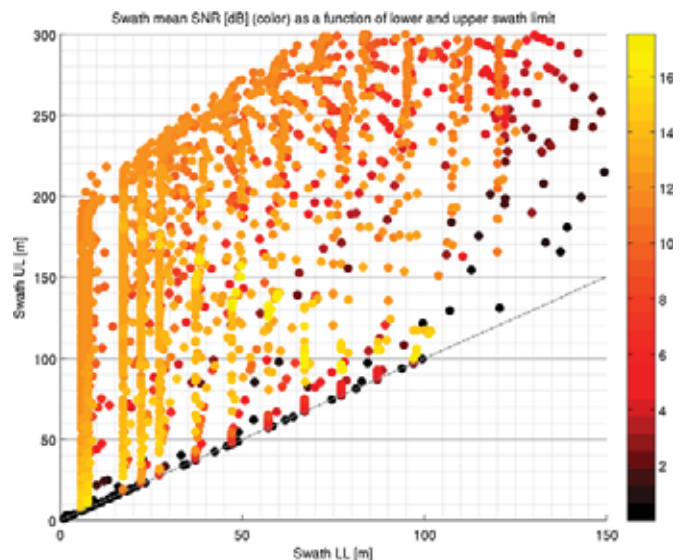


**Figure 4** Scatter plot showing brute force solutions for the deep water. Lower and upper swath limits are shown on the axes, i.e. the outer limits of where we can typically make a good sonar image.



In order to experimentally verify our method, we have collected sonar data using various sonar settings and vehicle altitudes. These data are collected in deep water, at about 196 meters, and in shallow water, at about 10 meters. For one of these measurements, we calibrate the SMURF model and use it to simulate the performance with the other settings for which we have measurements. This process is then repeated for all the measurements. Finally, the results and mean results are plotted, together with the actual measured performance, to illustrate the validity and accuracy of our method.

#### 4. RESULTS

With the brute force results we investigate the simulated performance of various sonar settings for the two different environments.

For the deep water environment, the plot in Figure 4 shows a scatter plot of the achieved lower and upper limits, and the mean swath SNR-level. The distinct vertical groupings reflect the lower swath limits, which are largely the same as the vehicle altitude. This is due to the vertical beam pattern of the receiver, which limits the minimum range to that of about 45 degrees down from the horizon. There are many solutions which result in good swath widths. There is also a weak trend indicating increasing SNR with decreasing swath width, which is expected as more energy is focused in a smaller area.

The plot in Figure 5 shows the swath width, i.e. the difference between the upper and lower limits, as a function of beam direction and beam width of the transmit beam, for a given altitude of 46 meters. If the beam is directed too high or too low the swath width suffers, but good results are achieved for many combinations of directions and beam widths. The results were largely the same for different altitudes, up until about 100 meters altitude, where the surface return arrives at the same time as the bottom return, and down to about 15 meters altitude, where the grazing angles gets very low at large range, and thus give less backscatter.

Figure 6 shows the model verification, which has each of the 30 measurements with different sonar settings as a function of the lower and upper swath limits on the range-axis. We can see that the measured swath limits in red match well with the simulated results, based on each of the other

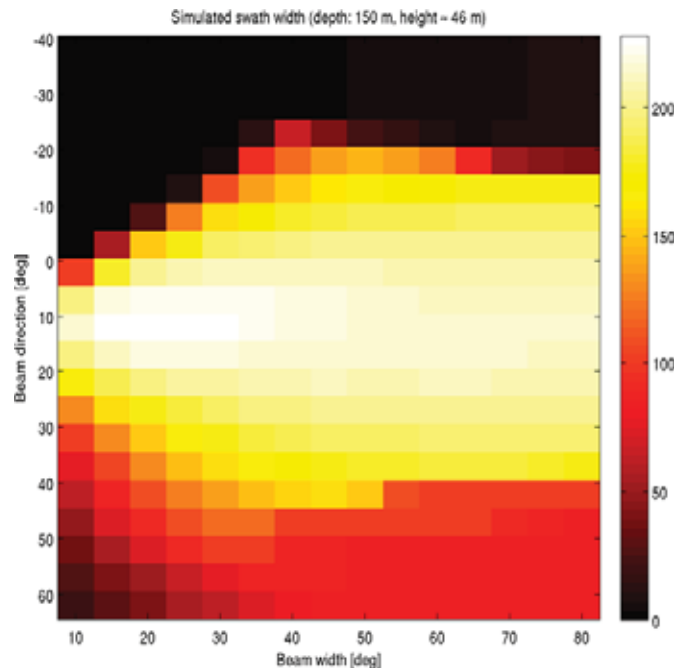


**Figure 5:** Simulated swath width for measured deep water environment (about 196 meters depth) for vehicle depth 150 meters, which was the best result. Comparable, good results are achieved for a wide vehicle depth interval.

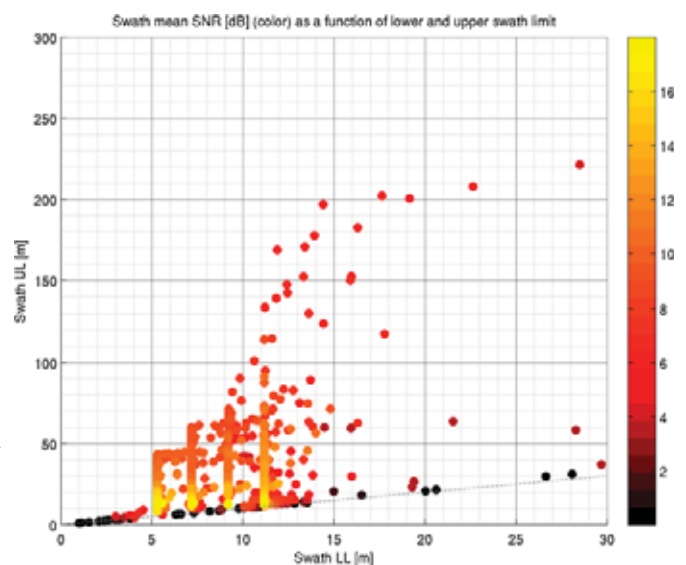


**Figure 7:** Scatter plot showing brute force solutions for the shallow water. Lower and upper swath limits are shown on the axes, i.e. the outer limits of where we can typically make a good sonar image.

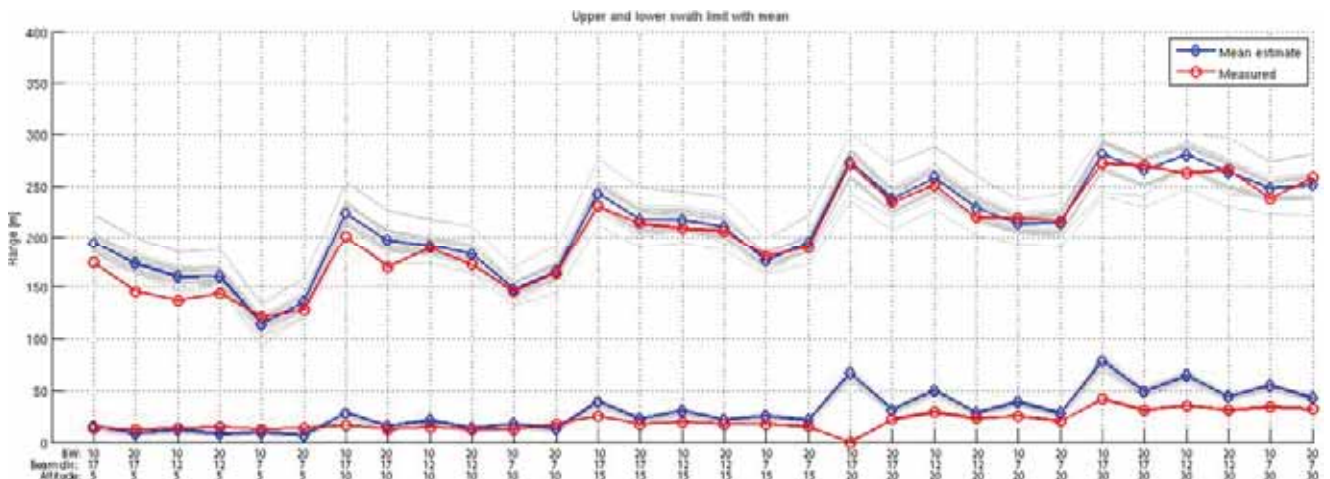
measurements. Each simulation result, i.e. the simulation of all the other settings based on the calibration from a single measurement, is added in light gray for an indication of the variance of the simulations.

For the shallow water environment, Figure 7 shows a scatter plot comparable to that of the deep water environment in Figure 4. The group of large swath widths is not as large in shallow water, and there is much to be gained from picking the right solution. Notice that we see the same distinct groups of lower swath limits, which correspond to the altitudes. Here it is more prominent that smaller swath widths allow for larger SNRs.

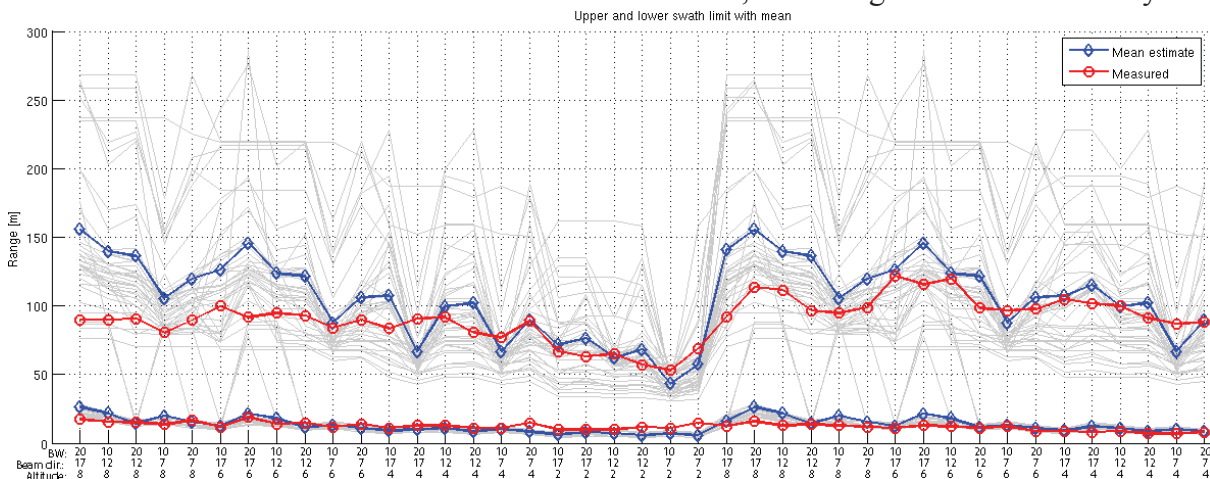
Figure 8 shows the simulated swath width for vehicle depths of 2, 4, 6 and 8 meters. The best results are achieved close to the surface with 8 meters altitude, or 2 meters depth, and a narrow beam directed slightly down from the horizon.

Figure 9 shows a model verification plot for the shallow water environment. The variance is larger than it was for the deep water environment, but most of the simulations are close to the measurements. The simulations that are very far off all originate from the same measurements, and is the result of outlier (and presumably wrong) bottom types and sea states found when calibrating the model.

Running a simple, unrefined implementation of the suggested, automated algorithm using a basic hill climbing search, we successfully found settings which are reasonable compared to the brute force solutions in about 97% of the cases for the deep water environment, and 85% of the cases for the shallow water environment. The runtime on a simple desktop computer for the deep water environment was lower than 5 seconds, while for the shallow water environment the average runtime was 34 seconds.



**Figure 6:** Model verification plot for the deep water measurements. It shows lower and upper limits (range-axis) for each measurement (horizontal axis). The red lines indicate the measured swath width for each measurement, while the blue lines indicate the average simulated swath width for each measurement based on calibration from each of the other measurements. The grey lines are the simulated results based on each of the measurements, indicating the variance visually.



**Figure 9:** Model verification plot for the shallow water measurements.

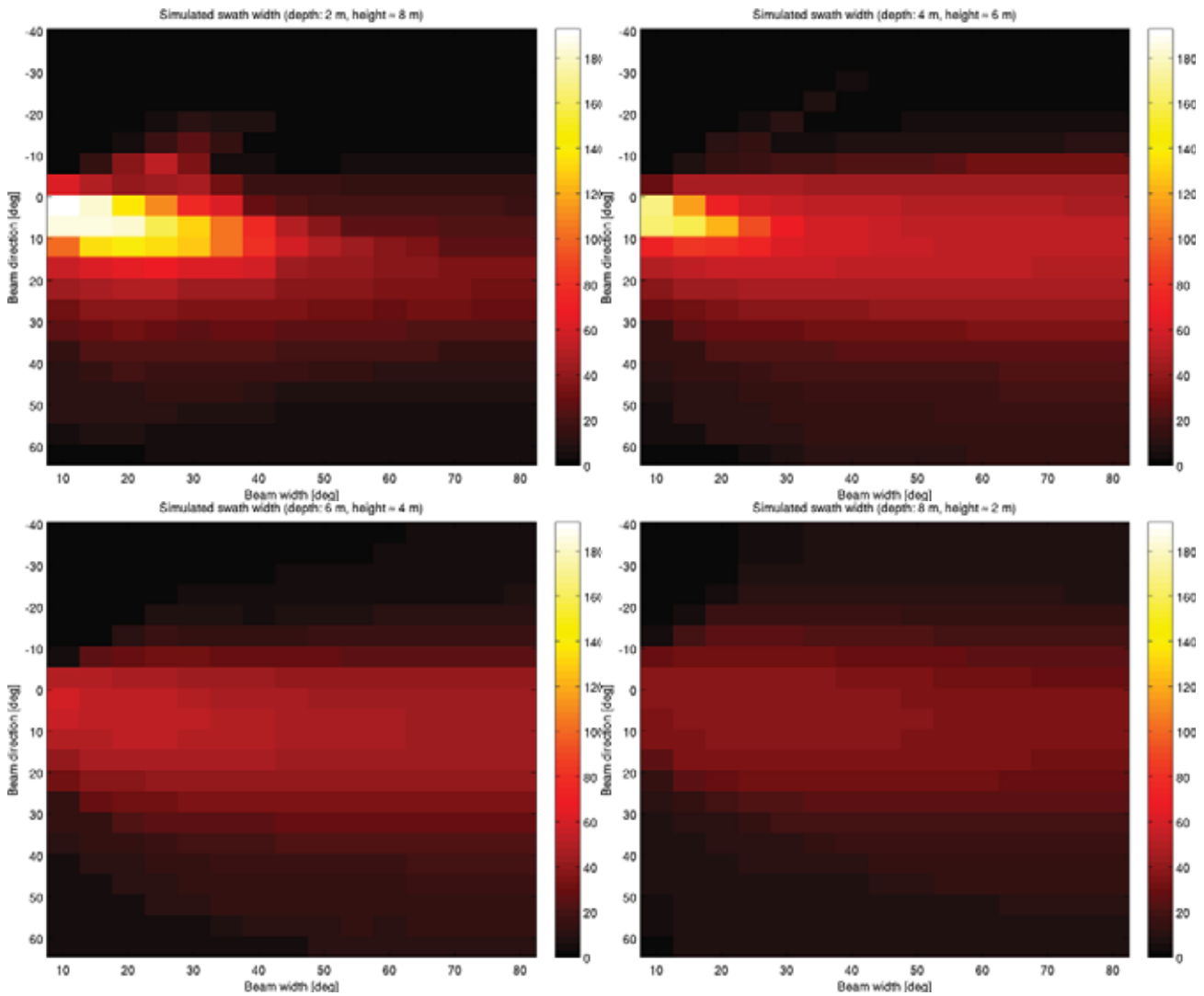


**Figure 8:** Simulated swath width for measured shallow water environment (about 10 meters depth) for vehicle depths 2, 4, 6 and 8 meters. In this case, the best swath widths are achieved with the vehicle close to the surface.

## 5. DISCUSSION AND CONCLUSION

Comparing the brute force search results based on the measurements from the deep and shallow water environments, we observe that the number of beam patterns with good performance is much smaller in shallow water with multipath presence. Thus, a standardized, fixed sonar setting may work well in deep water, even with changing environmental conditions, like sound speed profile and bottom type. In shallow water, however, the settings must be more precise and based on the current environmental conditions. The accuracy required for good performance in shallow water also increases the requirements on the simulation model. This means that it is important to accurately model the real antenna beam patterns, the sound velocity profile and the rest of the ocean environment.

We performed a model verification experiment, where we collected sonar data with different sonar settings in two different ocean environments. The results have some variance, particularly in the shallow water case, which is the most challenging one to simulate because of multipath presence. However, the simulations from each measurement seem to be relatively correct, meaning that the best measurement is also the best simulated result based calibration from any other measurement. This is a desirable quality when we want to be able to pick the best sonar settings, as it is sufficient to find improved settings, without necessarily predicting the actual performance with high accuracy.

Several challenges in adaptive sidescan sonar applications remain. Examples include rapidly adapting to very rough bathymetry, adapting to sloping sea floors, and imaging towards the shoreline, or even very steep, near-vertical bathymetry often found in fjords. We intend to address some of these challenges with further development of the adaptive sonar concept.

The quality of the sonar image is, of course, affected by more than the swath width given by the SNR [1]. More advanced prediction and estimation of sonar quality [6] will improve the robustness of this concept, and could also be expanded to autonomously improving the image quality.

The hill climber algorithm for adaptively improving sonar performance will be implemented in a HUGIN AUV ultimo 2013. This will be the real proof of concept for this method, as changing ocean environments require the adaptation to be performed in situ for the simulation to still be valid. Additionally, we will couple the result of this adaptation with automated mission planning and adaptive line spacing. This can improve range and area coverage rate autonomously, i.e. without involving the AUV operator.

## 6. ACKNOWLEDGEMENTS

Thanks to Kongsberg Maritime for providing a HUGIN vehicle and mission time to perform the data collection.

This work is more thoroughly documented in the master thesis *Environmentally Adaptive Sonar on an Autonomous Underwater Vehicle* [7].

## REFERENCES

- [1] **R. E. Hansen, H. J. Callow, T. O. Sæbø, S. A. V. Synnes**, “Challenges in Seafloor Imaging and Mapping with Synthetic Aperture Sonar,” *IEEE Trans. Geosci. Remote Sensing*, vol. 49, no 10, pp. 3677-3687, October 2011.
- [2] **T. O. Sæbø**, “Seafloor depth estimation by means of interferometric synthetic aperture sonar,” Ph. D. thesis, University of Tromsø, 2010.
- [3] **S. A. V. Synnes, R. E. Hansen, T. O. Sæbø**, “Assessment of shallow water performance using interferometric sonar coherence,” In *UAM 2009*, Nafplion, Greece, 2009.
- [4] **R. F. Hanssen**, “*Radar Interferometry: Data Interpretation and Error Analysis*”, Dordrecht, The Netherlands: Kluwer Academic Publishers, 2001.
- [5] **G. Carter, C. Knapp, A. Nuttall**, “Statistics of the estimate of the magnitudecoherence function”, *IEEE Transactions on Audio and Electroacoustics* vol. 21, no 4, pp. 388-389, 1973.
- [6] **R. E. Hansen, T. O. Sæbø**, “Towards Automated Performance Assessment in Synthetic Aperture Sonar,” in *Proceedings of Oceans 2013 MTS/IEEE*, Bergen, Norway, June 2013.
- [7] **O. J. Lorentzen**, “*Environmentally Adaptive Sonar on an Autonomous Underwater Vehicle*”, Master thesis, University of Oslo, November 2012.